固－気二相混合気におけるデトネーションの開始と伝播の数値シミュレーション

Numerical Simulations of Initiation and Propagation of Detonation in Gas-Solid 2-Phase Mixtures

O Krzysztof Benkiewicz, 青山学院大学理工学部機械創造工学科,〒157-8572 東京都世田谷区千歳台 6-16-1,
E-mail: kbenk@cow.me.aoyama.ac.jp
林 光一, 青山学院大学理工学部機械創造工学科, 〒157-8572 東京都世田谷区千歳台 6-16-1,
E-mail: hayashi@me.aoyama.ac.jp
O Krzysztof Benkiewicz, Aoyama Gakuin University, 6-16-1 Chitose, Setagaya, 157-8572 Tokyo
A. Koichi Hayashi, Aoyama Gakuin University, 6-16-1 Chitose, Setagaya, 157-8572 Tokyo

In the present paper the numerical model of the one-dimensional gas-solid two-phase chemically reacting flow is considered. The physical problem is modeled using the continuum mixture theory. Both continua are described by Euler equations and their mechanical and thermal interaction is represented by appropriate source terms. The numerical solution is obtained using time splitting technique and application of contemporary numerical methods. The model is applied for computation of initiation and propagation of detonation waves in the mixture consisting of aluminum particles suspended in the oxidizing atmosphere. The model of heterogeneous combustion, although simplified, includes production and destruction of several products of aluminum combustion. The computations show an influence of e.g. an initial solid phase concentration and particle diameter on the characteristic parameters of the detonation.

Introduction

Multi-phase flows are commonly observed in nature and industrial applications. Such phenomena as the bubbly flow in the pipes of nuclear reactor, detonation of the dust-methane-air mixture in coal mine or the motion of the volcanic ashes in the atmosphere are simple examples. These cases illustrate the great variety of time and spatial scales associated with such process as well as the diversity and complexity of the associated phenomena. Short, but of course incomplete list contains homogeneous and heterogeneous chemical reactions, vapor condensation, liquid evaporation, solid phase sublimation and/or decomposition under high temperature, heat transfer between both phases, etc.

The research on multi-phase flows is of great importance to the industry due to dust explosion hazards, its prevention, and mitigation of its effects. In many technological processes, the gas-solid or gas-liquid mixture is created during pneumatic transport of various materials. Such mixtures very often contain large amount of very fine particles and can be characterized by high surface/volume ratios. In case of flammable materials such mixture can have a strong ability to ignite and combust. For power-intensive substances detonation can be obtained and its destructive power observed.

Unfortunately the knowledge about laws that govern such phenomena is very limited due to high complexity of the phenomena and experimental difficulties. The problem of detonation in gas-solid two-phase mixtures has been analyzed by many researchers (see e.g. [1-8]). In many cases the resources, size of the apparatus, measurement methods and other aspects were strong limiting factors in such studies. Especially the high cost and time needed for experimental research are the “supporters” of the numerical model development.

Contemporary computer simulations are considered as a future supplement or even replacement for expensive and time-consuming experiments. They offer much higher flexibility and the possibility to “repeat” computational experiments in exactly the same conditions. They can be used for validation of theoretical models and investigate the influence of various parameters on the behavior of the whole system. It is also expected that numerical simulations can give additional information about modeled process that is difficult to obtain from experiments.

However each numerical experiment will depend on the set of physical parameters of modeled phenomena (see e.g. [5-8, 10-14]). These factors have to be validated and their influence on the results analyzed and compared with experimental data.

In this paper, we numerically investigate the influence of various parameters on the initiation and propagation of detonation in two-phase mixtures.

Modeling

The mixture consisting of solid particles suspended in oxidizing atmosphere is usually modeled using the continuum mixture theory. Various models and formulations can be found elsewhere (see e.g. [9-14]). In the present analysis the system of equations used by Benkiewicz et al. [14] (non-compressible solid phase, 2-temperatures, 2-velocities model) is employed. The one-dimensional case is considered. Although the particles are small and non-interacting their volume is not neglected. Such assumption, although very common, is not needed, because it does not simplify significantly the system of equation. It is also difficult to find reasonable criteria when this factor is negligible and when it is not.

The motion of each phase is described using Euler equations and their interaction is represented by appropriate source terms: the mass, momentum, and energy exchange. The system of equations can be written in a vector form as:

$$\frac{\partial U}{\partial t}+\frac{\partial F}{\partial z}=S$$

$$U=\begin{bmatrix} Y_1\cdot\rho_g \\ \dots \\ Y_k\cdot\rho_g \\ \rho_g \\ \rho_g\cdot u_g \\ \rho_g\cdot E_g \\ \rho_s\cdot\phi_s \\ \rho_s\cdot u_s\cdot\phi_s \\ \rho_s\cdot E_s\cdot\phi_s \\ n \end{bmatrix} \quad F=\begin{bmatrix} Y_1\cdot\rho_g\cdot u_g \\ \dots \\ Y_k\cdot\rho_g\cdot u_g \\ \rho_g\cdot u_g \\ \rho_g\cdot u_g^{\,2}+p_g \\ \left(\rho_g\cdot E_g+p_g\right)\cdot u_g \\ \rho_s\cdot u_s\cdot\phi_s \\ \rho_s\cdot u_s^{\,2}\cdot\phi_s \\ \rho_s\cdot E_s\cdot u_s\cdot\phi_s \\ n\cdot u_s \end{bmatrix} \qquad (1)$$

$$S=\begin{bmatrix} \xi_1\cdot\frac{1}{1-\phi_s}\cdot\Delta c\cdot\left(1-\frac{\rho_g}{\rho_s}\right)+\dot{\omega}_1 \\ \dots \\ \xi_k\cdot\frac{1}{1-\phi_s}\cdot\Delta c\cdot\left(1-\frac{\rho_g}{\rho_s}\right)+\dot{\omega}_k \\ \frac{1}{1-\phi_s}\cdot\Delta c\cdot\left(1-\frac{\rho_g}{\rho_s}\right) \\ \frac{1}{1-\phi_s}\cdot\left(\left(\frac{\Delta c}{2}-\delta\right)\cdot\left(u_g-u_s\right)+\Delta c\cdot\left(u_s-u_g\cdot\frac{\rho_g}{\rho_s}\right)\right) \\ \frac{1}{1-\phi_s}\cdot\left(\left(\frac{\Delta c}{2}-\delta\right)\cdot\left(u_g-u_s\right)\cdot u_s+\Delta c\cdot\left(E_s-E_g\cdot\frac{\rho_g}{\rho_s}\right)-h\cdot\left(T_g-T_s\right)\right) \\ -\Delta c \\ -\left(\left(\frac{\Delta c}{2}-\delta\right)\cdot\left(u_g-u_s\right)+\Delta c\cdot u_s\right) \\ -\left(\left(\frac{\Delta c}{2}-\delta\right)\cdot\left(u_g-u_s\right)\cdot u_s+\Delta c\cdot E_s-h\cdot\left(T_g-T_s\right)\right) \\ f \end{bmatrix}$$

where:

T	–	independent time coordinate,
z	–	independent spatial coordinate,
k	–	number of species,
$Y_1..Y_k$	–	mass fraction of species, $\sum_{i=1}^{k} Y_i = 1$
ρ_g	–	gas phase density,
u_g	–	gas phase velocity,
E_g	–	total gas phase energy (thermal and kinetic), $E_g(T)=\left(\sum_{i=1}^{k} Y_i\cdot\left(\Delta h_{f\,298_i}+\int_{298}^{T} C_{pg_i}(T)\cdot dT\right)\right)-\frac{p_g}{\rho_g}+\frac{u_g^2}{2}$
Δh_{f298i}	–	formation enthalpy at $T=298$ [K] for i-th component,
$C_{pgi}(T)$	–	specific heat at constant pressure at T for i-th component,
p_g	–	gas phase pressure, $p_g=\rho_g\cdot\frac{B}{M}\cdot T_g$
B	–	universal gas constant,
M	–	gas phase molar weight,
T_g	–	gas phase temperature,
ρ_s	–	solid phase density,
ϕ_s	–	solid phase volume fraction, $\phi_s=\frac{solid\ \ phase\ \ volume}{total\ \ volume}$
u_s	–	solid phase velocity,
E_s	–	total solid phase energy (thermal and kinetic), $E_s(T)=\Delta h_{f\,298_s}+\int_{298}^{T} C_{vs_i}(T)\cdot dT+\frac{u_s^2}{2}$
Δh_{f298s}	–	formation enthalpy at $T=298$ [K] for solid phase,
$C_{vs}(T)$	–	specific heat at constant volume at T for solid phase,
T_s	–	solid phase temperature,
n	–	particle number density (number of particles divided by the total volume of the mixture),
Δc	–	mass exchange between both phases,
δ	–	drag force coefficient,
H	–	heat transfer coefficients,
$\xi_1...\xi_k$	–	fractions of the total mass exchange between both phases that are transferred to each species, $\sum_{i=1}^{k}\xi_i=1$
$\dot{\omega}_i$	–	species source/sink due to homogeneous chemical reactions, $\sum_{i=1}^{k}\dot{\omega}_i=0$
F	–	particle source/sink function (here: $f=0$),

As one can find from the system of equations (1) it describes the mixture consisting of solid/liquid particles suspended in k-component gaseous atmosphere. The gas phase obeys the ideal equation of state, but the species thermal properties are functions of the temperature (see Kee et al. [15]). The viscous, diffusion and heat conduction terms are omitted. Solid phase internal energy and specific heat are also temperature-dependent and already include all phase transitions (melting, evaporation). The interaction terms Δc, δ, and h depend on the flow field properties and particle diameter d. The particles are assumed to be spherical and uniform in size within the computational cell. The average particle diameter d can be calculated from:

$$d=\left(\frac{6\cdot\phi_s}{\pi\cdot n}\right)^{\frac{1}{3}} \tag{2}$$

The drag force d and heat transfer coefficient are calculated using the following formulas:

$$\delta=\frac{3}{4}\cdot\frac{\phi_s}{d}\cdot C_x\cdot\rho_g\cdot\left|u_g-u_s\right| \tag{3}$$

$$h=6\cdot\phi_s\cdot\frac{Nu\cdot\lambda_g}{d^2} \tag{4}$$

where the drag force coefficient C_x is calculated form equations proposed by Henderson [16], and Nu is a Nusselt number obtained from Hoglund et al. [17]. λ_g is a heat conduction coefficient in gas and can be calculated using relations described in Kee et al. [15].

The mass transfer Δc describes the mass exchange between both phases and is a problem-specific term. Its form is strongly dependent on the material characteristics and accessible experimental data. Unlike the other parameters and functions this term is associated with the very high uncertainty and introduces the largest inaccuracy into the model. In the case of homogeneous chemical reactions there are many popular, reliable and well-verified detailed chemical kinetics sub-models. There are also some global models that in certain conditions sufficiently describe the chemistry without significant increase of computational costs. For the heterogeneous chemical reactions, evaporation or condensation process such models either do not exist or are very rough approximation to the experimental data. This is caused mainly by much higher complexity and very limited knowledge about heterogeneous chemical reactions, as well as experimental difficulties in such studies.

A good example of "difficult" material is aluminum and its oxidation in various atmospheres (see [5-8, 13-14, 18-26]). Many research show that aluminum burns in gaseous phase and that this process should or is controlled by the diffusion. On the other hand aluminum particles easily cover with an oxide that protects particle from further oxidation. This covering oxide layer may crack due to thermal expansion of the aluminum core and disrupt the d^2-law that usually describes diffusion-controlled combustion/evaporation. This is accompanied by other phenomena such as phase transition in metal, aluminum oxide condensation on the aluminum droplets or non-existence of aluminum oxide in gaseous phase. This causes high scatter of combustion related data such as ignition temperature or burning law (compare e.g. [5, 18-26]).

There is also the possibility to employ pure kinetic model such as in Liang et al. [26]. Unfortunately the reference [26] does not quote the whole data about considered reactions (forward and backward reaction rate coefficients) and used for the

computations.

As one can find from the published results the aluminum combustion is quite complex. For our purposes we apply very simple empirical combustion law used by [5, 8, 13]. The induction time is modeled by the assigned ignition temperature T_{ign}, while the mass transfer (solid/liquid aluminum consumption rate) is described as:

$$\Delta c = \frac{3 \cdot \phi_s \cdot \rho_s}{\tau} \cdot \left(1 + 0.276 \cdot \sqrt{\mathrm{Re}}\right) \quad \text{for} \quad T_s \geq T_{ign} \quad (5)$$

where Re is a relative Reynolds number based on particle diameter d and the velocity difference between both phases ($|u_g - u_s|$). τ is a characteristic time of combustion defined by:

$$\tau = K \cdot \frac{d_0^{\,2}}{X_{O2}^{\,0.9}} \quad (6)$$

where $K=4 \cdot 10^6$ [s/m^2] (for aluminum), d_0 is initial diameter of particles and X_{O2} is the initial mole fraction of O_2 in the gas phase. This law is very simple but computations by Borisov et al. [5], Khasainov et al. [13] and Veyssière et al. [8] were very successful.

In this research we assume that the Eqs. (5) and (6) are valid independently on the possible reaction mechanism and that they describe the solid/liquid aluminum consumption rate. The considered possible reaction products are oxygen (O_2), aluminum monoxide (AlO), aluminum oxide (Al_2O_3) and gaseous aluminum (Al). The last two can contribute to the gas phase internal energy and specific heat, but due to the lack of transport data it is assumed that they do not contribute to the gas viscosity and heat conductivity. Although aluminum oxide does not exist in gas phase it is assumed that it can be present in the form of very fine particles that behave as a gas and are treated as a gaseous component. Aluminum can appear in gaseous form by evaporation of liquid aluminum and when there is not enough oxygen to burn it with. Depending on the gas phase properties (temperature), aluminum vapor can be burnt into Al_2O_3 or AlO. This reaction is assumed to be infinitely fast.

Additionally it is assumed that if the gas phase exceeds some limiting value T_{decomp}, then the aluminum oxide decomposes into aluminum monoxide and oxygen:

$$Al_2O_3 \rightarrow 2AlO + \frac{1}{2}O_2 \quad (7)$$

This effect was directly included by Borisov et al. [5] in the equation for heat release because it is endothermic one and prevents from obtaining excessive temperatures. In our approach the heat of reaction is not used explicitly, since the internal energy includes formation enthalpy and the aluminum oxide decomposition is assumed to be proportional to the term:

$$\dot{\omega}_{decomp} \approx 1 - \exp\left(-\frac{T_g - T_{decomp}}{\Delta T}\right) \quad \text{for} \quad T_g \geq T_{decomp} \quad (8)$$

This formula may seem to be in some contradiction to Arrhenius type law, but one has to remember that this equation does not describe here any chemical kinetics. The reaction (7) is endothermic and it is included in order to introduce some feedback effect (but present in reality!) and to limit the maximum temperature of the combustion products. For high overheating (T_g-T_{decomp}) the equation (8) tends to be some asymptotic value and does not increase the stiffness of the source terms, but still plays effectively the role of temperature moderator. The parameters in Eq. (8) have yet to be confirmed in our computations and compared with experimental data.

Computational technique

The set of equations is solved using the time splitting technique because it allows for application of the most suitable or easily accessible solvers for each problem. The Strang-type interleaving of PDE and ODE solvers is employed:

$$U^{n+1} = L_{PDE}^{\frac{\Delta t}{2}} L_{ODE}^{\Delta t} L_{PDE}^{\frac{\Delta t}{2}} \left(U^n\right) \quad (9)$$

where the operator L_{PDE} describes the solution of homogeneous PDE:

$$L_{PDE}: \quad \frac{\partial U}{\partial t} + \frac{\partial F}{\partial z} = 0 \quad (10)$$

and L_{ODE} describes the solution of the source terms using ODE solver:

$$L_{ODE}: \quad \frac{dU}{dt} = S \quad (11)$$

Simple analysis of governing equations shows that conservative part of Eqs. (1) can be split into the "gaseous" and "solid" part because the parameters of both phases do not depend on each other. This allows for application of different methods for each phase.

For the gas phase the Harten-Yee flux modified TVD method with MINMOD limiter is applied, because it has been found to give the most satisfactory results for pure gas phase flow problems (sharp shocks and small smearing of the discontinuities). For the purpose of this research the whole eigenstructure of the system of equations for the multi-component gas phase has been obtained. The details can be found elsewhere [27-29].

More problems can be found in the case of solid phase equations since they do not contain phase pressure. They have the complete system of real eigenvalues, but do not have independent eigenvectors and following this, this system of equations is hyperbolically degenerate. In order to be able to use here contemporary high-resolution TVD numerical methods we have to find the numerical method that do not use eigenvectors, but still can give TVD-type solution. For our case the Godunov-type MUSCL-Hancock (van Leer) TVD numerical method (see Toro [30]) and a "good" approximate Riemann solver are applied. Figure 1 presents the initial data and Fig. 2 shows possible solution patterns of the Riemann problem.

Since this system of equations is hyperbolically degenerate then one obtains only 2 waves (defined by velocities u_l and u_r) characteristic to the states on the left (U_l) and right (U_r) side. If one considers expansion, then $u_l<u_r$ and the particles move away from each other. If $u_l>0$ and $u_r>0$ (Fig. 2a) then the solution is the left state: $F^*=F(U_l)$. Similarly, if $u_l<0$ and $u_r<0$ (Fig. 2b) then the solution is the right state: $F^*=F(U_r)$. If $u_l<0$ and $u_r>0$ (Fig. 2c) then the solution is the vacuum $F^*=0$. If we now consider compression then $u_l>u_r$ and the particle are approaching each other. If $u_l>0$ and $u_r>0$ (Fig. 2d) then the solution is the left state: $F^*=F(U_l)$. Similarly, if $u_l<0$ and $u_r<0$ (Fig. 2e), then the solution is the right state: $F^*=F(U_r)$. The case when $u_l>0$ and $u_r<0$ (Fig. 2f) is the most difficult and we propose the following solution:

$$F^* = F\left(U_l\right) + F\left(U_r\right) \quad (12)$$

Similar solvers can be found in Collins et al. [31] and Saurel et al. [32].

This Riemann problem solver may be used only for limited number of cases. Such solver will give the incorrect solution if particles have high inertia and do not follow the gas motion, or if the gas pressure is very low. In such cases the drag force is not able to decelerate particles fast enough (motion relative to the gas). If one considers two identical clouds of particles moving against each other with the same velocity then the continuous approach will give solid wall made of particles, while in practice both clouds may cross each other almost without interaction. This is because the continuum model uses some integral variables (e.g. concentration and momentum), while in reality each particle has its own mass and vector of velocity. In addition two crossing clouds of particles have higher energy when considered as a discrete one than when assumed as continuum. The difference is the kinetic energy that "disappears" when the average momentum

in the cell is used. If the interaction (drag) from the gas phase is sufficiently high then the particles are easily decelerated and aforementioned problems are not so sevre (but still do exist).

Saurel et al. [32] proposed splitting the particles into left-moving and right-moving families. This automatically solves the crossing clouds of particles and their energy problem. Unfortunately this approach introduces additional equations and in the multi-dimensional case it may be more complicated procedure. It may be prohibitive if one wants to model more real cases and, for example, to consider many groups of particles with different initial diameters.

The ordinary system of equations (11) describing the interaction between both phases is solved using 4-th order Runge-Kutta method. It is effective and very simple in implementation, but it also low accuracy method. In a newer version of the code the popular and reliable VODE (DVODE) procedure from CHEMKIN-II package is used.

Results

In these studies we analyze influence of various factors on the calculated propagation of the shocks and their transition to detonation waves. Shock-tube like experiment is considered. In all cases the same strong shock (direct initiation) is used as the initial condition (see Table 1.).

Parameter:	Left side:	Right side:
Pressure [bar]:	100.0	1.0
Temperature [K]:	2000.0	300.0
Velocity [m/s]:	0.0	0.0
Gas phase composition Y_i [1/1]:		
O_2	1.0	1.0
Al(g)	0.0	0.0
AlO	0.0	0.0
Al_2O_3(g)	0.0	0.0
Solid phase:	Aluminum	
Grid size [mm]:	2.0	
Boundary conditions:	Reflective	Non-reflective

Table 1. Initial conditions.

The grid system is moving with shock/detonation front so if the shock front is close to the right boundary then the whole grid moves ("jumps") to the right. As an effect the grid no longer contains the initial point of symmetry and the left boundary condition changes to non-reflective one.

The example of the detonation front profile at $t=25.0$ [ms] is shown in Figs. 3-7. The initial concentration of solid phase is $c_{s0}=500$ [gm/m^3], the particle diameter is equal $d_0=5$ [μm], the ignition temperature is $T_{ign}=1350$ [K] and the decomposition temperature: $T_{decomp}=3250$ [K]. The peak pressure is equal to $p_g=48.1$ [bar] and the detonation wave velocity is equal to $D=1625.6$ [m/s] which is within the range of theoretical and experimental values obtained by Borisov et al. [5]. The wave is not steady state, but it is oscillating around some average value. The sudden drop in the solid phase temperature (Fig. 4 – dashed line) and velocity (Fig. 5 – dashed line) is the result of the complete consumption of the aluminum particles. The composition of the products (Fig. 7) shows that the aluminum oxide (green line) is created just behind the detonation front, where the temperature is below the decomposition temperature T_{decomp}. This leads to fast increase of the temperature and then, to the change of the combustion mechanism. Farther behind the detonation front the primary combustion product is aluminum monoxide (red line). It stabilizes the temperature of the products close to the decomposition temperature. The decomposition reaction has small influence on the gas phase composition mainly due to a small difference between the gas temperature and the decomposition temperature. Because of high concentration of oxygen the aluminum vapor does not appear in the combustion products because it is immediately burnt into either Al_2O_3 or AlO.

These results are the basis for further comparisons. Figure 8 shows the positions of the detonation fronts for initial concentrations c_{s0} ranging from *400* to *2000* [gm/m^3]. Higher initial solid phase concentration means that more energy can be released due to chemical reactions and stronger wave can be obtained. For example, for $c_{s0}=400$ [gm/m^3] the peak pressure is equal to $p_g=43.97$ [bar], while for $c_{s0}=2500$ [gm/m^3] the peak pressure increases to $p_g=67.63$ [bar]. From the Fig. 9 it seems that it approaches some maximum value at about $c_{s0}=2500\text{-}3000$ [gm/m^3]. For higher initial concentrations it may decrease as an effect of reduced or insufficient concentration of oxidizer, as well as increased drag force from incompletely burned particles and higher heat sink to the solid phase. Figure 10 presents the dependence of detonation velocity on the initial solid phase concentration. The increase of solid phase concentration slows down the detonation wave. It is caused by increased drag force and heat sink to the solid phase due to higher number of particles. Following this also the development of the detonation wave is prolonged. The heat exchange between both phases is of major importance because it has direct influence on the heating and ignition of solid aluminum. Similar simulations with larger particles ($d_0=15$ [μm] in diameter) do not lead to detonation because the particles have high thermal inertia. Additionally in the case of larger particles the heat transfer is much slower. In these conditions particle do not reach the ignition temperature and the detonation cannot develop. This is in agreement with experimental results. For example Borisov et al. [5] noticed that even very strong initiator (*125* gm-TNT charge) was not able to initiate detonation in the aluminum-oxygen mixture if the particle size exceeded *10* [μm]. Unfortunately for initial concentrations less than *400* [gm/m^3] we were not able to obtain transition to detonation. The reasons have to be investigated in our future research.

The influence of initial particle diameter on the detonation wave propagation at $t=5$ [ms] is shown in Figs. 11-13. Two cases are analyzed: $d_0=5$ [μm] (red) and $d_0=10$ [μm] (blue line). The initial solid phase concentration was $c_{s0}=1000$ [gm/m^3]. In both cases the pressure profiles (Fig. 11) are almost the same. Slightly higher and peak pressure in the case of larger particles may be attributed to higher solid phase concentration (see Fig. 13) in this region. This peak in solid phase concentration is caused by the moving detonation wave and associated gas-solid interaction due to the drag force. Small difference in the position of the detonation front suggests that particle diameter has minor influence on the detonation velocity, providing that it is sufficiently small to allow for development of the detonation. In case of larger particles we can observe small induction period just behind the initial jump in gas phase temperature (Fig. 12). This time and space are needed for heating the particles to ignition temperature. In case of small particles the induction period is not visible and it suggests that much finer grid is needed to obtain good resolution of the induction region. For example some Automatic Mesh Refinement method may be used in this region. In both cases the phase transition of the aluminum (melting) is very fast and not visible in the solid phase temperature profiles (not presented here).

In the present simulations the correct description of the combustion is crucial to the proper modeling of the detonation process. Unfortunately there is a high scatter of aluminum combustion related data in the literature (see e.g. [5, 22-24]). For example the aluminum ignition temperature can vary from about *900* [K] to over *2350* [K], depending on the source in the literature. The lower the ignition temperature then easier ignition and faster the development of the detonation should be observed. Figures 14-16 show the influence of the ignition temperature on the computed detonation wave profiles. The red and blue lines are the solutions when ignition temperature is $T_{ign}=1000$ [K] and $T_{ign}=1350$ [K], respectively. From these figures one can conclude that the choice of the ignition temperature has in practice no influence on the

propagation of the detonation, but it has influence on its development. If the ignition temperature is too high, then the solid phase is not able to reach this point and the detonation cannot develop (for current initiation condition). Similar simulations with $T_{ign}=1500$ [K] do not lead to the development of the detonation wave.

Since the ignition temperature has small effect on the detonation, the influence of other effects is considered. The aluminum oxide decomposition reaction is not very well understood. In the literature one can find that the temperature at which Al_2O_3 decomposes into AlO and O may vary from about 3250 [K] to 4000 [K] (see e.g. [5, 21, 25]). The formula of the chemical kinetic reaction rate is also not known. Here we try to analyze the influence of the decomposition temperature T_{decomp} and decomposition rate on the basic properties of the detonation wave. Figures 17-19 show the pressure, temperature and velocity profiles (respectively) at $t=10$ [ms]. The initial solid phase concentration is $c_{s0}=500$ [gm/m^3], the particle diameter $d_0=10$ [μm] and the ignition temperature is $T_{ign}=1350$ [K]. Three cases are considered:

(a) $T_{decomp}=3250$ [K] (green line),
(b) $T_{decomp}=3500$ [K] (red line),
(c) $T_{decomp}=3500$ [K] and the aluminum oxide decomposition rate 100 times higher than in (b) (blue line).

The computations were performed using modified version of the code that solves the ordinary system of equations (Eq. (11)) using highly accurate VODE (DVODE) subroutine from CHEMKIN-II package. The results show that increase in the decomposition temperature leads to faster detonation wave because more aluminum is burned to aluminum oxide and more energy is released in the system. The increase of the gas temperature is obvious since the T_{decomp} is automatically the limiting temperature in the system. If the system exceeds slightly T_{decomp}, then the main combustion product is AlO and Al_2O_3 decomposes. This leads to the decrease of the temperature. If it drops below T_{decomp} then the aluminum oxide again becomes the main combustion product and the temperature may again grow. This process is clearly visible in Fig. 20 that shows O_2 (blue), Al_2O_3 (green) and AlO (red line) mass fractions for the case (c). These oscillations are inherently connected to the combustion and decomposition modeling and probably are not related to the oscillations in Figs. 17-19. The period of pressure oscillations (Fig. 17) for example is longer than gas composition oscillations (Fig. 20). The peak pressure oscillates between *40* and *70* [bar] and the detonation wave propagation is not steady state. Although the peak pressure for case (c) is higher than for case (b) (see Fig. 17), the increase of the decomposition rate has no visible influence on the computations, because in both cases the pressure oscillates in the same range of values.

Unfortunately it was not possible to analyze the cases when T_{decomp} was higher than *3500* [K]. In such cases the gas phase temperature and heat transfer from gas to the solid are very high and the particle temperature exceeds the boiling point. The pressure correction of the boiling point and small overheating included in our model are insufficient to prevent from such occurrence. This problem has to be solved in our future studies.

Conclusions

The computer simulations of one-dimensional gas-solid two-phase flows have been performed. The case of initiation and propagation of the detonation wave is considered and the influence of various parameters on these process – analyzed. The results show, that the major influence on the computed solutions have the initial solid phase concentration and the combustion model. The initial particle diameter and ignition temperature are found to have minor influence on the propagation of the detonation, but they are limiting factors for its development. Too big particles or too high ignition temperature may prevent from the transition to the detonation even if the initiator is quite strong. On the other hand the decomposition temperature and following this change of the combustion mechanism have stronger influence on the system because it automatically limits the energy release in the combustion process. The decomposition reaction by itself is probably not very important but the change of the main combustion product from aluminum oxide to aluminum monoxide at the decomposition temperature is crucial to the proper modeling of the detonation process. The chemical reaction model although simple is only rough approximation to the real process and more precise chemical kinetics is needed for the analysis of practical cases.

References

[1] Wolanski, P., Kauffman, C. W., Ural, E., Nicholls, J. A., Van Dyk, R., “Shock initiated combustion of grain dust”, Proceedings of the International Symposium on Grain Dust, Manhattan, Kansas (1979)

[2] Gardner, B. R., Winter, R. J., Moore, M. J., “Explosion development and deflagration to detonation transition in coal dust/air suspensions”, Proceedings of 21st International Symposium on Combustion, The Combustion Institute, Pittsburgh (1986), pp. 335-343,

[3] Zhang, F., Grönig, H., "Two-headed detonation in particle-oxidizing gas flow", Physics of Fluids, Vol. 4 (1992), pp. 2308-2315

[4] Zhang, F., Grönig, H., "Spin detonation in reactive particles-oxidizing gas flow", Physics of Fluids, Vol. A3 (8) (1991), pp. 1983-1990

[5] Borisov, A., Khasainov, B. A., Saneev, E. L., Fomin, I. B., Khomik, S. V., Veyssière, B., "On the Detonation of Aluminum Suspension in Air and in Oxygen" in Borisov, A. A. (eds.), "Dynamic Structure in Gaseous and Dispersed Media", Kluwer Academic Press (1991), pp. 215-253,

[6] Veyssière, B., "Structure of the Detonation in Gaseous Mixtures Containing Aluminum particles in Suspension" in "Dynamics of Explosions", Progress in Astronautics and Aeronautics, Vol. 106 (1986), pp. 522-544

[7] Veyssiere, B., "Ignition of Aluminum Particles in a Gaseous Detonation" in Bowen, J. R. (eds.); "Shock Waves, Explosions, and Detonations", Progress in Astronautics and Aeronautics, Vol. 87 (1983), pp. 362-375

[8] Veyssière, B., Khasainov, A., "A Model for Steady, Plane, Double-Front Detonations (DFD) in Gaseuous Explosive Mixtures with Aluminum Particles in Suspension", Combustion and Flame, 85 (1991), pp. 241-253

[9] Stewart, H. B., Wendroff, B., “Two-Phase Flow: Models and Methods”; Journal of Computational Physics, Vol. 56 (1984), pp. 363-409

[10] Smirnov, N. N., "Combustion and detonation in multi-phase media. Initiation of detonation in dispersed-film systems behind a shock wave", International Journal on Heat and Mass Transfer, Vol. 31, No. 4 (1988), pp. 779-793

[11] Zhong, S., Deng, X., Li, G., He, D., Li, X., "Numerical simulation of bituminous dust/air mixture explosion in a Hartmann bomb", Proceedings of 15th International Symposium on Combustion Process, Zakopane, Poland (1997)

[12] Smirnov, N. N., Nikitin, V. F., Klammer, J., Klemens, R., Szatan, B., Wolanski, P., Legros, J. C., "Theoretical modeling of turbulent combustion of dust-air mixtures", Archivum Combustionis, Vol. 17, No. 1-4 (1997), pp. 27-36

[13] Khasainov, A., Vessiere, B., "Steady, Plane, Double-Front Detonations in Gaseous Detonable Mixtures Containing a Suspension of Aluminum Particles" in "Dynamics of Explosions", Progress in Astronautics and Aeronautics, Vol. 114 (1988), pp. 284-299

[14] Benkiewicz, K., Hayashi, A. K., “One-dimensional numerical modeling of gas-solid mixtures ignition using continuum mixture theory with “compressible solid” and “non-compressible solid”

sub-models" (submitted to Archivum Combustionis)
[15] Kee, R. J., Miller, J. A., Jefferson, T. H., "CHEMKIN General-Purpouse, problem-independent, transportable FORTRAN chemical kinetics code package", SAND80-8003 (1980)
[16] Henderson, C. B., "Drag Coefficients of Spheres in Continuum and Rarefied Flows", AIAA Journal, Vol. 14, No. 6 (1976), pp. 707-708
[17] Hoglund, R. F., Carlson, D. J., "Particle Drag and Heat Transfer in Rocket Nozzles", AIAA Journal, Vol. 2, No. 11 (1964), pp. 1980-1984
[18] Law, C. K., "A Simplified Theoretical Model for the Vapor-Phase Combustion of Metal Particles", Combustion Science and Technology, Vol. 7 (1973), pp. 197-212
[19] King, M. K., "Modeling of single particle aluminium combustion in CO_2-N_2 atmospheres", Seventeenth Symposium (International) on combustion (1978), pp. 1317-1328
[20] Bucher, P., Yetter R. A., Dryer, F. L., Parr, T. P., Hanson-Parr, D. M., Vicenzi, E. P., "Flame structure measurement of single, isolated aluminium particles burning in air", Twenty-Sixth Symposium (International) on combustion (1996), pp. 1899-1908
[21] Bucher, P., Yetter, R., Dryer, F., Vicenzi, E., Parr, T., Hanson-Parr, D., "Condensed-phase Species Distributions about Al Particles Reacting in Various Oxidizers", Combustion and Flame, Vol. 117 (1999), pp. 351-361
[22] Merzhanov, A. G., Grigorjev, Yu. M., Gal'chenko, Yu. A., "Aluminum Ignition", Combustion and Flame, Vol. 29 (1977), pp. 1-14
[23] Friedman, R., Macek, A., "Ignition and Combustion of Aluminum Particles in Hot Ambient Gases", Combustion and Flame, Vol. 6 (1962), pp. 9-19
[24] Fedorov, A. V., Khmel', T. A., Fomin, V. M., "Non-equilibrium model for steady detonations in aluminum particles-oxygen suspensions", Shock Waves, Vol. 9 (1999), pp. 313-318
[25] Price, E. W., "Combustion of Metalized Propellants", AIAA (1983)
[26] Liang, Y., Beckstead, M. W., "Numerical Simulation of Quasi-Steady, Single Aluminum Particle Combustion in Air", AIAA Paper 89-0254 (1998), pp. 1-9
[27] Harten, A., "High Resolution Schemes for Hyperbolic Conservation Laws", Journal of Computational Physics, 49 (1983), pp. 357-393
[28] Yee, H. C., "Construction of Explicit and Implicit Symmetric TVD Schemes and Their Applications", Journal of Computational Physics, 68 (1987), pp. 151-179
[29] Hirsch, C., "Numerical Computation of Internal and External Flows", Vol. 1-2, John Willey & Sons (1995)
[30] Toro, E. F., "Riemann Solvers and Numerical Methods for Fluid Dynamics", Spriger-Verlag (1997)
[31] Collins, J. P., Ferguson, R. E., Chien, K. -Y., Kuhl, A. L., Krispin, J., Glaz, H. M, "Simulation of shock-induced dusty gas flows using various models", AIAA Paper 94-2309 (1994)
[32] Saurel, R., Daniel, E., Loraud, J. C., "Two-Phase Flows: Second-Order Schemes and Boundary Conditions", AIAA Journal, Vol. 32, No. 6 (1994), pp. 1214-1221

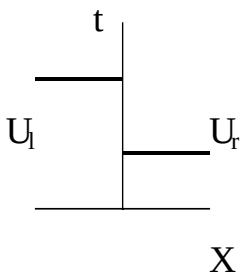

Figure 1. Riemann problem for solid phase.

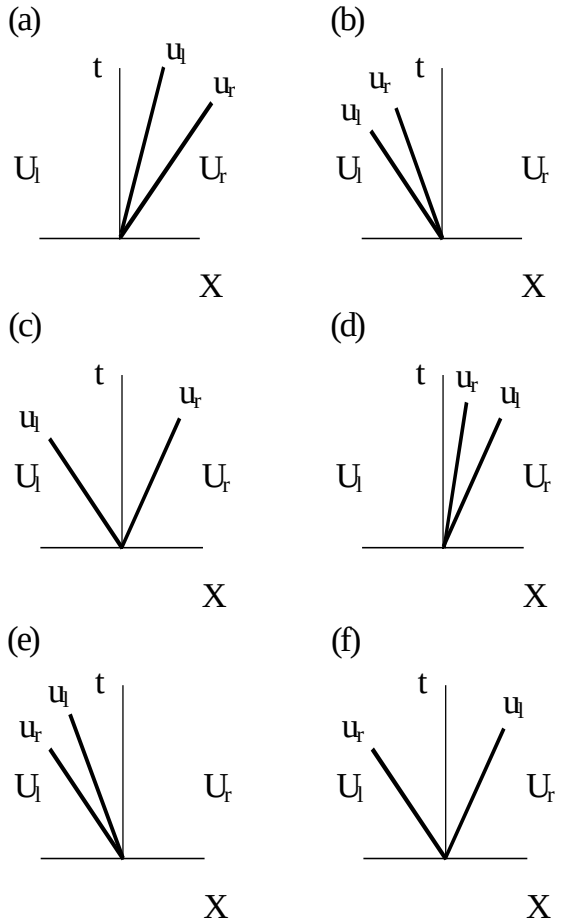

Figure 2. Solution patterns for solid phase Riemann problem.

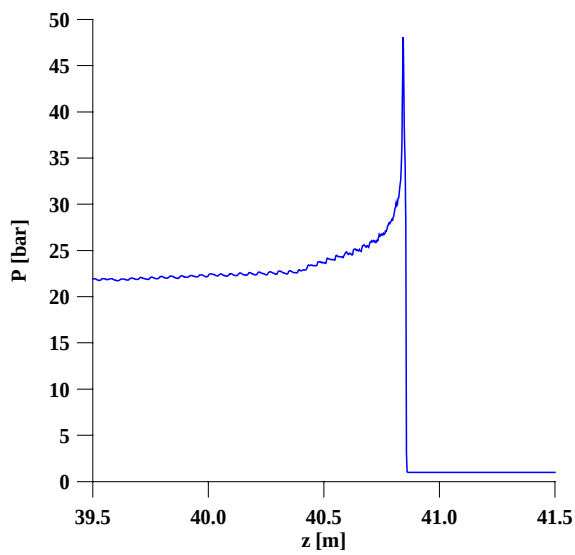

Figure 3. Detonation front: pressure profile (t=25 [ms], c_{s0}=500 [gm/m^3], d_0=5 [μm]).

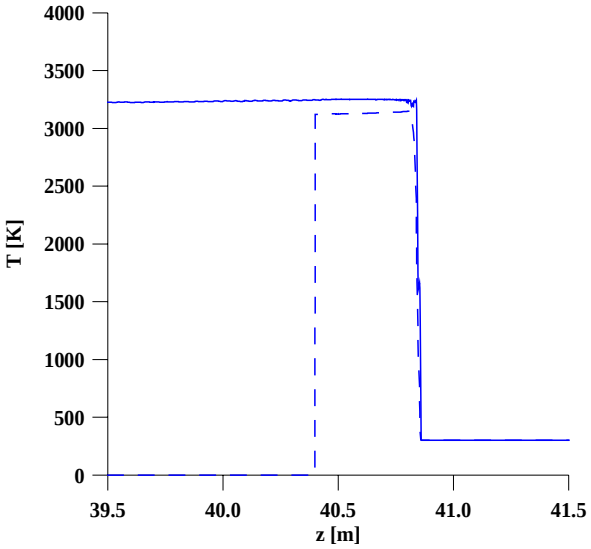

Figure 4. Detonation front: gas (solid) and solid phase temperature profile (dashed line) (t=25 [ms], c_{s0}=500 [gm/m^3], d_0=5 [μm]).

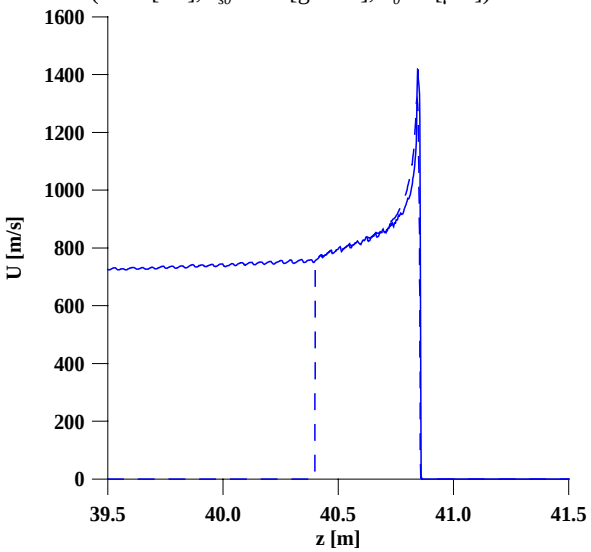

Figure 5. Detonation front: gas (solid) and solid phase velocity profile (dashed line) (t=25 [ms], c_{s0}=500 [gm/m^3], d_0=5 [μm]).

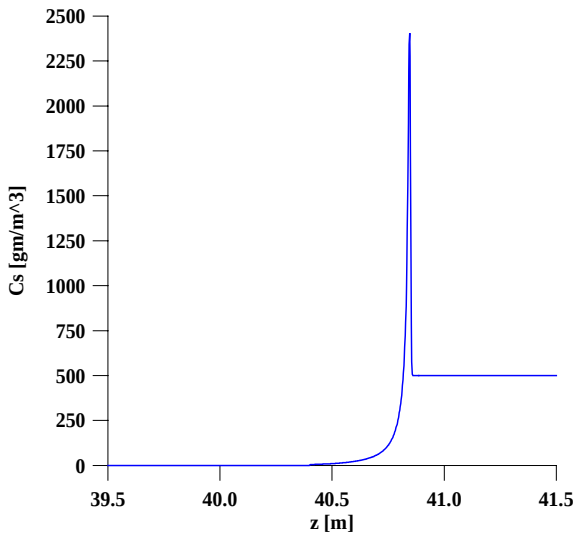

Figure 6. Detonation front: solid phase concentration profile (t=25 [ms], c_{s0}=500 [gm/m^3], d_0=5 [μm]).

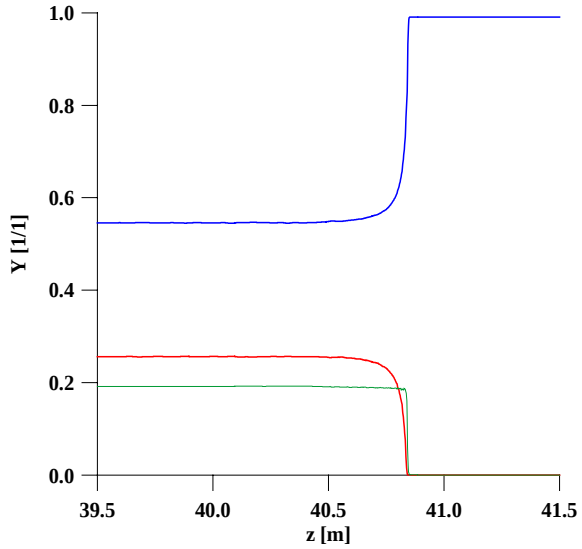

Figure 7. Detonation front: gas phase composition profiles (O_2 – blue, Al_2O_3 – green, AlO – red line) (t=25 [ms], c_{s0}=500 [gm/m^3], d_0=5 [μm]).

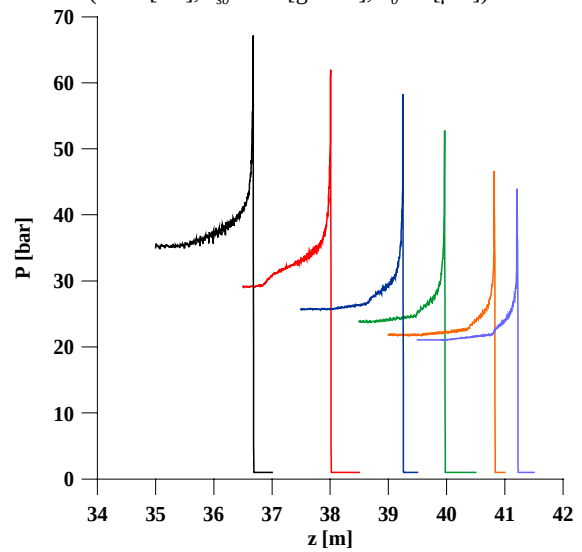

Figure 8. Pressure profiles for various initial concentrations of the solid phase (t=25 [ms], c_{s0}=400 (light blue), 500 (orange), 750 (green), 1000 (dark blue), 1500 (red) and 2000 [gm/m^3] (black), d_0=5 [μm]).

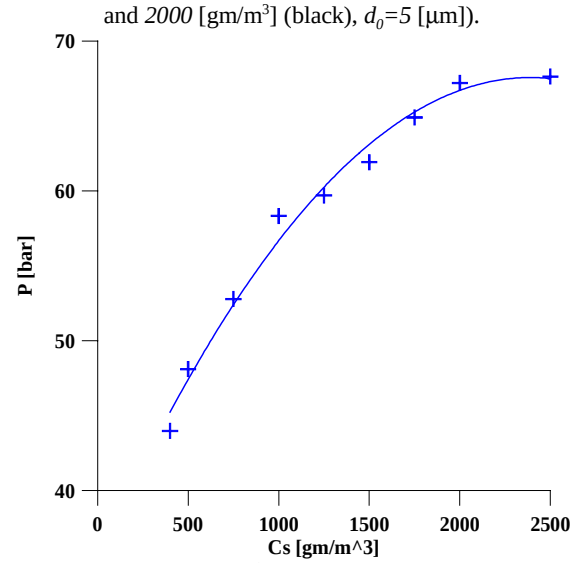

Figure 9. Dependence of the peak pressure on the initial solid phase concentration (t=25 [ms], c_{s0}=400-2500 [gm/m^3], d_0=5 [μm]).

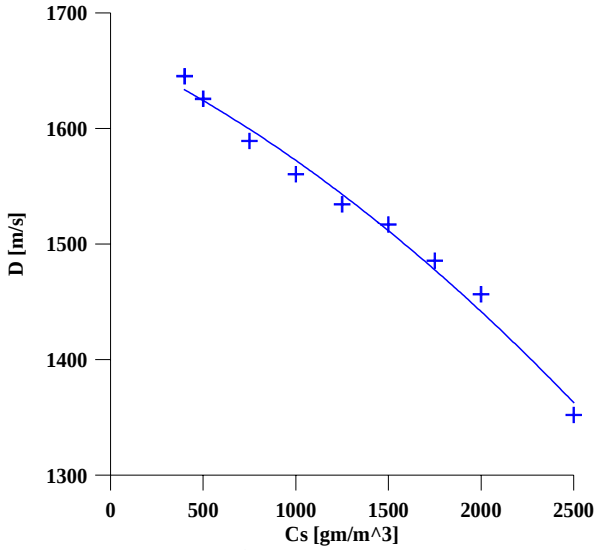

Figure 10. Dependence of the detonation velocity on the initial solid phase concentration (t=25 [ms], c_{s0}=400-2500 [gm/m^3], d_0=5 [μm]).

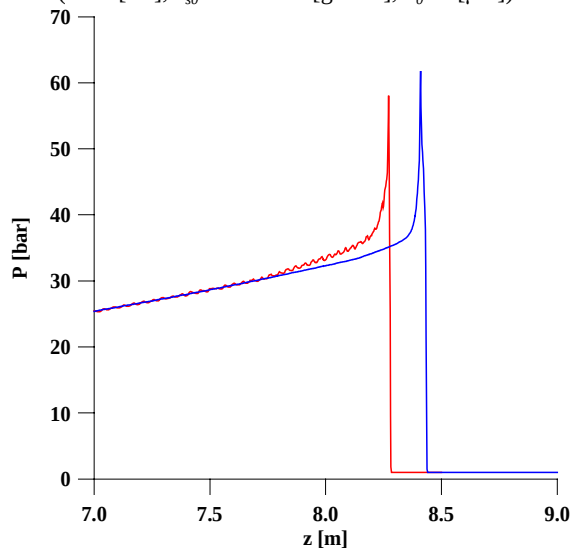

Figure 11. Comparison of the pressure profiles for various initial particle diameters (t=5 [ms], c_{s0}=1000 [gm/m^3], d_0=5 [μm] (red line), d_0=10 [μm] (blue line)).

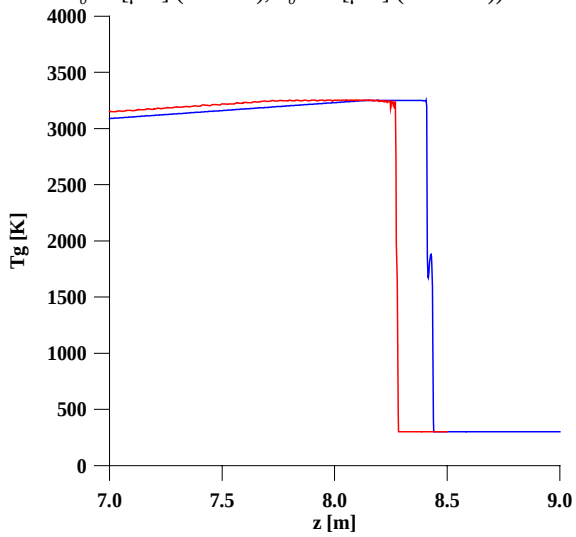

Figure 12. Comparison of the temperature profiles for various initial particle diameters (t=5 [ms], c_{s0}=1000 [gm/m^3], d_0=5 [μm] (red line), d_0=10 [μm] (blue line)).

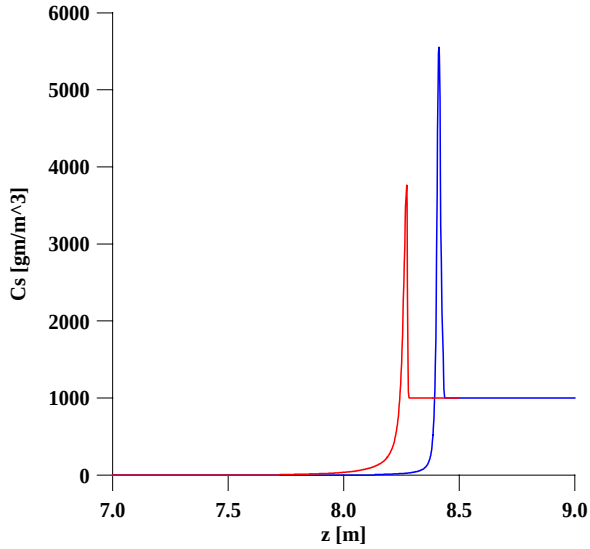

Figure 13. Comparison of the solid phase concentration profiles for various initial particle diameters (t=5 [ms], c_{s0}=1000 [gm/m^3], d_0=5 [μm] (red line), d_0=10 [μm] (blue line)).

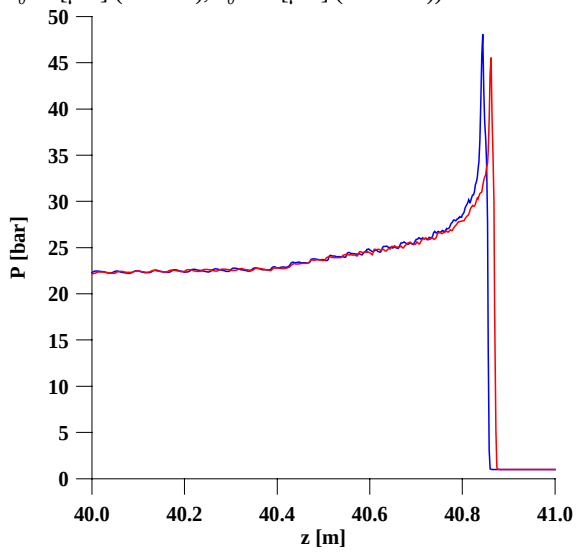

Figure 14. Comparison of the pressure profiles for various ignition temperatures (t=25 [ms], c_{s0}=500 [gm/m^3], d_0=5 [μm], T_{ign}=1000 [K] (red line), T_{ign}=1350 [K] (blue line)).

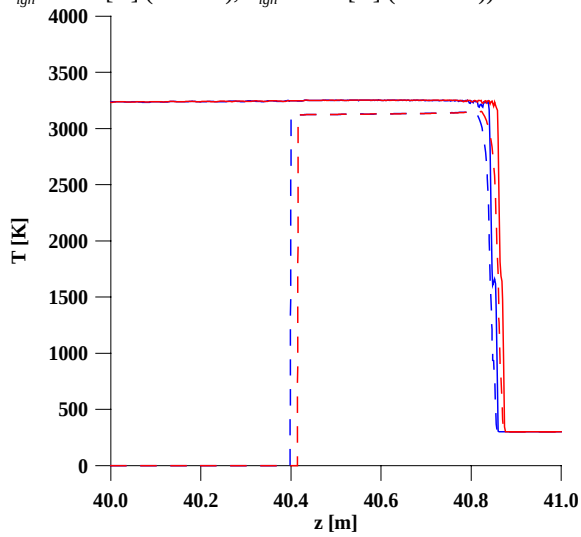

Figure 15. Comparison of the temperature profiles for various ignition temperatures for gas (solid) and solid phase (dashed line) (t=25 [ms], c_{s0}=500 [gm/m^3], d_0=5 [μm], T_{ign}=1000 [K] (red line), T_{ign}=1350 [K] (blue line)).

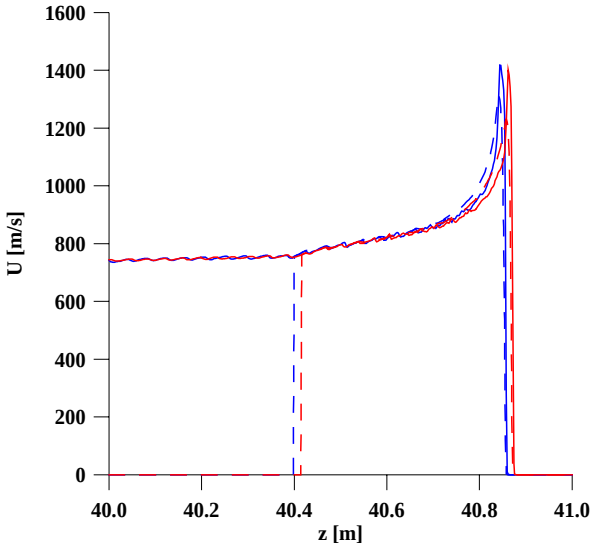

Figure 16. Comparison of the velocity profiles for various ignition temperatures for gas (solid) and solid phase (dashed line) (t=25 [ms], c_{s0}=500 [gm/m^3], d_0=5 [μm], T_{ign}=1000 [K] (red line), T_{ign}=1350 [K] (blue line)).

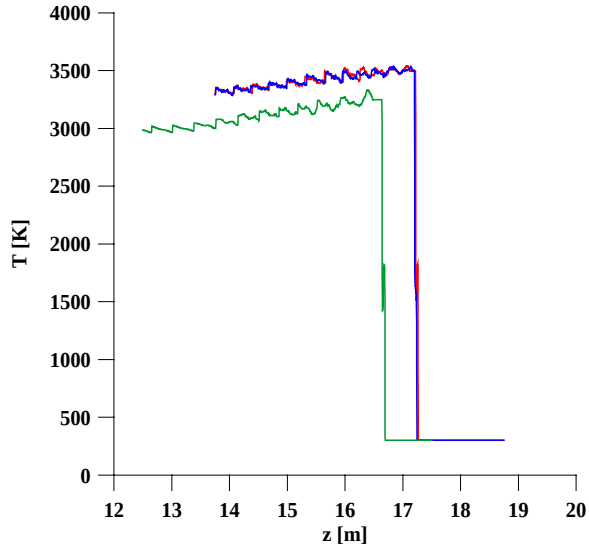

Figure 18. Comparison of the temperature profiles for various decomposition temperatures and rates (t=10 [ms], c_{s0}=500 [gm/m^3], d_0=10 [μm], (a) T_{decomp}=3250 [K] (green), (b) T_{decomp}=3500 [K] (red), (c) T_{decomp}=3500 [K] and high decomposition rate).

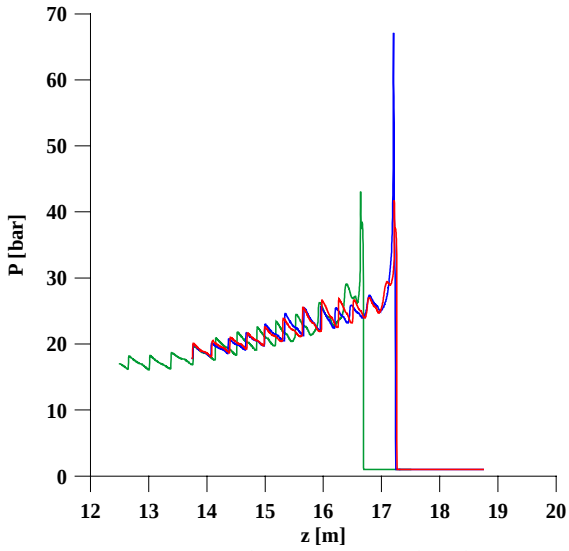

Figure 17. Comparison of the pressure profiles for various decomposition temperatures and rates (t=10 [ms], c_{s0}=500 [gm/m^3], d_0=10 [μm], (a) T_{decomp}=3250 [K] (green), (b) T_{decomp}=3500 [K] (red), (c) T_{decomp}=3500 [K] and high decomposition rate).

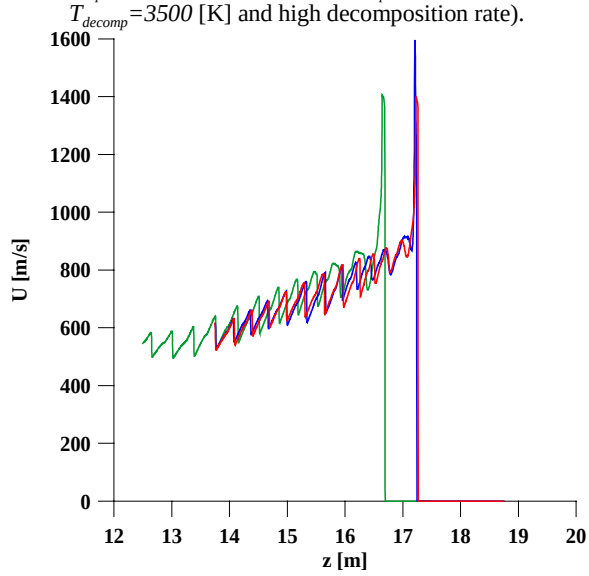

Figure 19. Comparison of the velocity profiles for various decomposition temperatures and rates (t=10 [ms], c_{s0}=500 [gm/m^3], d_0=10 [μm], (a) T_{decomp}=3250 [K] (green), (b) T_{decomp}=3500 [K] (red), (c) T_{decomp}=3500 [K] and high decomposition rate).

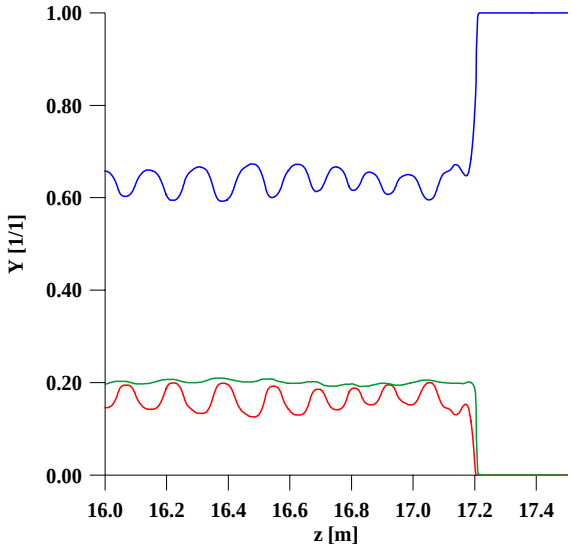

Figure 20. Profiles of the gas phase composition (O2 – blue, Al_2O_3 – green, AlO – red line) ($t=10$ [ms], $c_{s0}=500$ [gm/m^3], $d_0=10$ [μm], $T_{decomp}=3500$ [K] and high decomposition rate).